Journal of Catalysis **209,** 237–244 (2002)
doi:10.1006/jcat.2002.3619

Organotin–Oxometalate Coordination Polymers as Catalysts for the Epoxidation of Olefins

Marta Abrantes,* Anabela Valente,† Martyn Pillinger,† Isabel S. Gonçalves,† João Rocha,† and Carlos C. Romão*,[1]

*Instituto de Tecnologia Química e Biológica da Universidade Nova de Lisboa, Quinta do Marquês, EAN, Apt. 127, 2781-901 Oeiras, Portugal; and †Department of Chemistry, University of Aveiro, Campus de Santiago, 3810-193 Aveiro, Portugal

Received February 4, 2002; revised March 21, 2002; accepted March 21, 2002

The polymeric organotin–oxometalates $[(n\mathrm{Bu_3Sn})_2MO_4]$ (M = Mo, W) were used as catalysts in the liquid-phase epoxidation of cyclooctene at 35–75°C. Using 70% *tert*-butyl hydroperoxide (TBHP) as oxidant, the molybdenum(VI) compound is much more active than the tungsten(VI) analogue, yielding cyclooctene oxide as the only product, in 88% yield, after 24 h. The solid catalyst could be recycled without measurable loss of activity. For both catalysts, activity increased markedly by using 30% aqueous H_2O_2 instead of TBHP, with no detectable loss of selectivity. The best results were obtained by adding a noncoordinating solvent to give heterogeneous triphasic systems (aqueous H_2O_2, organic, and solid). For example, with $[(n\mathrm{Bu_3Sn})_2MoO_4]$ and dichloromethane, cyclooctene oxide was obtained in quantitative yield within 6 h at room temperature. Experiments were also carried out using other substrates (cyclododecene, 1- and 2-octene). The catalyst precursors were fully characterized in the solid state, including powder XRD, FTIR, and Raman spectroscopy, MAS NMR (^{13}C, ^{119}Sn), and EXAFS spectroscopy. © 2002 Elsevier Science (USA)

Key Words: **molybdenum; tungsten; tin; coordination polymer; heterogeneous catalysis; cyclooctene; epoxidation; *t*-butyl hydroperoxide; hydrogen peroxide; solvent effects.**

INTRODUCTION

One of the main goals of crystal engineering is the synthesis of novel microporous materials using both inorganic and organic components (1–4). A particularly appealing strategy is to use covalent coordinative bonds and organic or inorganic ligands as links between metal atoms. The aim is to construct two- or three-dimensional (2-D or 3-D) coordination polymers that mimic conventional zeolites in that they exhibit reversible guest exchange and possibly selective catalytic activity. Several research groups are studying organotin–cyanometalate coordination polymers with the general formula $[(R_m\mathrm{Sn^{IV}})_x\{M(\mathrm{CN})_n\}_y]$ (R = Me, Et, or Ph; M = Fe, Co, Ru, Os, Cu, Mo, or W) (5–11). A common feature of all compounds in this class is the polymeric M–C≡N–Sn–N≡C–M chains which intersect to build up frameworks with various topologies. The choice of R group determines the specific organotin–cyanometalate structure, while the topology of the framework is also determined by the number of CN groups per metal atom. Some of these compounds exhibit intercrystalline reaction chemistry (10, 11). For example, $[(\mathrm{Fe^{III}Cp_2})\ (\mathrm{Me_3Sn})_3\mathrm{Fe^{II}(CN)_6}]$ was synthesized by the direct intercalation of $[(\mathrm{Me_3Sn})_3\mathrm{Fe^{II}(CN)_6}]$ with ferrocene ($\mathrm{Fe^{II}Cp_2}$) (10).

While attempting to crystallize the coordination polymer $[(\mathrm{Me_3Sn})_3\mathrm{Mo(CN)_8}]$ from the reaction of Me_3SnCl with $K_4[\mathrm{Mo(CN)_8}]_2 \cdot H_2O$ (in air), Fischer and co-workers unexpectedly obtained crystals of the organotin–oxomolybdate $[(\mathrm{Me_3Sn})_2MoO_4]$ (12). This compound has a layered structure built up of tetrahedral MoO_4 and trigonal–bipyramidal Me_3SnO_2 units. It was subsequently found that a broad range of compounds of the type $[(R_3E)_2MO_4]$ (R = Me, Et, nPr, nBu, or Ph; E = Sn or Pb; M = Mo or W) are accessible by precipitation from aqueous solution. These compounds are related to the polymeric complexes $[\mathrm{Me_3SnO}M\mathrm{O_3}]$ [M = Re (13) or Tc (14)], which have zigzag-chain structures. Very recently, organotin–oxovanadates $[\mathrm{Me_3SnVO_3}]$ and $[(\mathrm{Me_2Sn})_4V_2O_9]$ with novel 3-D network structures were also reported (15). To the best of our knowledge, the catalytic properties of these coordination polymers have yet to be investigated. Such compounds should be interesting because of the variety of mixed metal oxides that have found catalytic applications in numerous reactions (16). SnO_2-supported molybdenum oxides, for example, have been employed as catalysts for the oxidation of methanol to formaldehyde (17–19), and ethanol oxidation to either acetaldehyde (20, 21) or acetic acid (22, 23).

In the present work the compounds $[(n\mathrm{Bu_3Sn})_2MO_4]$ (M = Mo or W) have been examined as catalysts or catalyst precursors for the epoxidation of olefins by *tert*-butyl hydroperoxide (TBHP) or aqueous H_2O_2. In addition to varying the type of oxidant, the effects of temperature and solvent have been studied. The precursor materials were characterized by powder X-ray diffraction (XRD), IR and Raman spectroscopy, solid-state MAS NMR (^{13}C and

[1] To whom correspondence should be addressed. Fax: 351 21 4411277. E-mail: ccr@itqb.unl.pt.

0021-9517/02 $35.00

^{119}Sn), and X-ray absorption fine structure (XAFS) spectroscopy at the Mo and Sn *K*-edges.

EXPERIMENTAL

General Methods and Instrumentation

Powder XRD data were collected on a Philips X'pert diffractometer using CuK_α radiation filtered by Ni. Microanalyses were performed at the ITQB (Oeiras). Infrared spectra were recorded on a Unican Mattson Mod 7000 FTIR spectrometer using KBr pellets. Raman spectra were recorded on a Bruker RFS 100/S FT Raman spectrometer using a 1064-nm excitation of the Nd/YAG laser. Room-temperature solid-state ^{119}Sn NMR and ^{13}C NMR spectra were recorded at 149.21 and 100.62 MHz, respectively, on a (9.4 T) Bruker Avance 400 spectrometer. ^{119}Sn MAS NMR spectra were recorded with a 3.5-μs ^{1}H 90° pulse, 3-ms contact time, 9.5-kHz spinning rate, and 4-s recycle delays. Chemical shifts are quoted in parts per million from $Sn(CH_3)_4$. ^{13}C CP MAS NMR spectra were recorded with a 4.5-μs ^{1}H 90° pulse, 2-ms contact time, 8-kHz spinning rate, and 4-s recycle delays. Chemical shifts are quoted in parts per million from TMS. The precursors $Na_2MoO_4 \cdot 2H_2O$ and $Na_2WO_4 \cdot 2H_2O$ were obtained from Aldrich and recrystallized before use.

Mo *K*-edge and Sn *K*-edge X-ray absorption spectra were measured at room temperature in transmission mode on beamline BM29 at the ESRF (Grenoble), operating at 6 GeV in 2/3 filling mode with typical currents of 180–190 mA. One scan was performed for each sample and set up to record the preedge region at 5 eV steps and the post-edge region in 0.025- to 0.05-Å^{-1} steps, giving a total acquisition time of ca. 40 min per scan. The order-sorting double Si(311) crystal monochromator was detuned to give 40% harmonic rejection. Solid samples were diluted with BN and pressed into 13-mm pellets. Ionization chamber detectors were filled with Kr to give 30% absorbing I_o (incidence) and 70% absorbing I_t (transmission). The programs EXCALIB and EXBACK (SRS Daresbury Laboratory, UK) were used in the usual manner for calibration and background subtraction of the raw data. EXAFS curve-fitting analyses, by least-squares refinement of the non-Fourier filtered k^3-weighted EXAFS data, were carried out using the program EXCURVE [version EXCURV98 (24)] using fast-curved wave theory (25). Phase shifts were obtained within this program using *ab initio* calculations based on the Hedin Lundqvist/von Barth scheme.

Preparation of Catalysts

[(nBu$_3$Sn)$_2$MoO$_4$] (**1**):nBu$_3$SnCl (3.25 g, 10 mmol) was dissolved in a mixture of water (6 ml) and acetone (27 ml). A saturated aqueous solution of $Na_2MoO_4 \cdot 2H_2O$ (1.21 g, 5 mmol in 8 ml H_2O) was added dropwise with magnetic stirring to the nBu$_3$SnCl solution. A white precipitate formed immediately and stirring was continued for 5 min. After that, the precipitate was filtered, washed thoroughly with water, and dried in air at 100°C, giving 3.3 g (90%). Anal. Found: C 38.68, H 7.10. Calcd. for $C_{24}H_{54}O_4MoSn_2$ (740.02): C 38.95, H 7.36%. Selected IR (KBr, ν cm^{-1}): 2960 (s), 2922 (s), 2873 (m), 2856 (m), 1506 (w), 1464 (m), 1417 (w), 1377 (m), 1342 (w), 1292 (w), 1261 (w), 1182 (w), 1155 (w), 1078 (w), 1047 (w), 1007 (w), 966 (w), 883 (m), 850 (s), 810 (vs), 744 (m), 696 (s), 667 (s), 611 (w), 513 (w). ^{119}Sn CP MAS NMR: δ = 20.2 and 17.9. ^{13}C CP MAS NMR: δ = 29.1, 28.6, 28.2, 27.8, 27.2, 26.9, 20.8, 20.4, 20.2, 14.8, 14.5, 13.9.

[(nBu$_3$Sn)$_2$WO$_4$] (**2**):nBu$_3$SnCl (3.24 g, 10 mmol) was dissolved in a mixture of water (6 ml) and acetone (27 ml). A saturated aqueous solution of $Na_2WO_4 \cdot 2H_2O$ (1.65 g, 5 mmol in 10 ml H_2O) was added dropwise with magnetic stirring to the nBu$_3$SnCl solution. A white precipitate formed immediately and stirring was continued for 5 min. After that, the precipitate was filtered, washed thoroughly with water, and dried in air at 100°C, giving 3.7 g (90%). Anal. Found: C 34.65, H 6.59. Calcd. for $C_{24}H_{54}O_4Sn_2W$ (827.81): C 34.82, H 6.57%. Selected IR (KBr, ν cm^{-1}): 2960 (vs), 2922 (vs), 2873 (s), 2856 (s), 1512 (w), 1464 (s), 1417 (w), 1377 (m), 1342 (w), 1292 (w), 1250 (w), 1182 (w), 1155 (w), 1078 (m), 1049 (w), 1003 (w), 964 (w), 883 (m), 850 (s), 815 (vs), 744 (m), 696 (s), 669 (s), 613 (w), 513 (w). ^{119}Sn CP MAS NMR: δ = −13.0 and −17.2. ^{13}C CP MAS NMR: δ = 29.1, 28.8, 28.6, 28.1, 27.2, 26.9, 21.0, 20.6, 20.4, 14.9, 14.5, 14.2, 13.8.

*Catalytic Epoxidations with **1** and **2** as Catalysts*

The liquid-phase catalytic oxidations were performed under air atmosphere (atmospheric pressure) in a reaction vessel equipped with a magnetic stirrer and immersed in a thermostated oil bath. A 1% molar ratio of catalyst/substrate (7.2 mmol cyclooctene and 72 μmol complex) and a substrate/oxidant molar ratio of 0.5 were used with 10 ml solvent. Samples were withdrawn periodically and analyzed using a gas chromatograph (Varian 3800) equipped with a capillary column (SPB-5, 20 m × 0.25 mm × 0.25 μm) and a flame ionization detector. Cyclooctene epoxide was quantified using a calibration curve and undecane as internal standard (added after the reaction).

RESULTS AND DISCUSSION

Synthesis and Characterization of Organotin–Oxometalates

The organometallic coordination polymers [(nBu$_3$Sn)$_2$$MO_4$] with M = Mo (**1**) and W (**2**) were obtained as analytically pure colorless precipitates by addition of a saturated aqueous solution of $Na_2MO_4 \cdot 2H_2O$ to a saturated

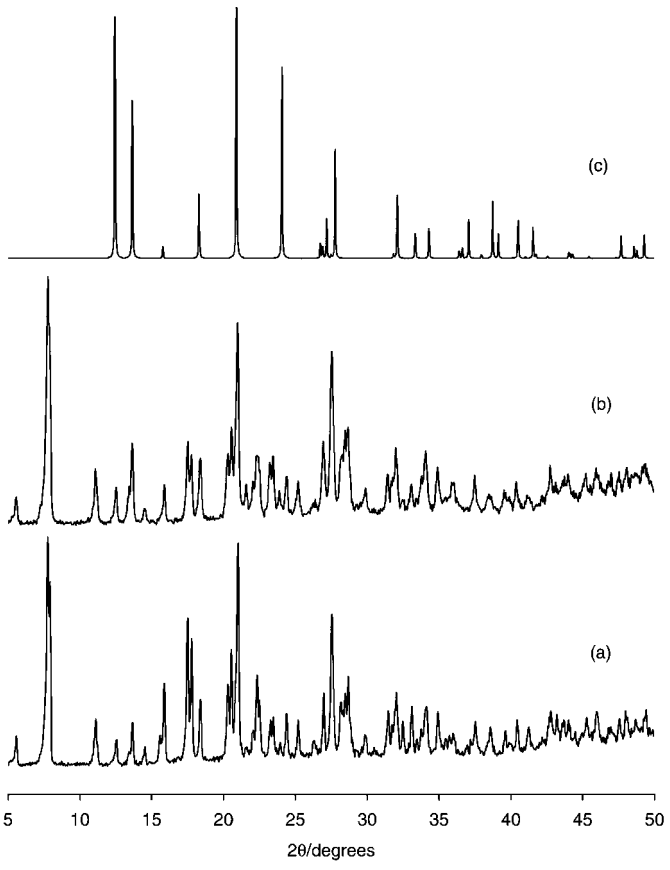

FIG. 1. Powder XRD patterns of (a) $[(n\mathrm{Bu_3Sn})_2\mathrm{MoO_4}]$ (**1**) (experimental), (b) $[(n\mathrm{Bu_3Sn})_2\mathrm{WO_4}]$ (**2**) (experimental), and (c) $[(\mathrm{Me_3Sn})_2\mathrm{MoO_4}]$ (simulated).

solution of $n\mathrm{Bu_3SnCl}$ at room temperature:

$$2n\mathrm{Bu_3SnCl} + \mathrm{Na_2}[M\mathrm{O_4}] \xrightarrow[\mathrm{Me_2CO}]{\mathrm{H_2O}} [(n\mathrm{Bu_3Sn})_2M\mathrm{O_4}]\downarrow + 2\mathrm{NaCl}, \qquad [1]$$

where $M = \mathrm{Mo}$ (**1**), W (**2**). The products were recovered by filtration, washed with water, and air-dried at 100°C for several hours. Compounds **1** and **2** are isostructural, as evidenced by the similarity of the powder XRD patterns (Fig. 1). These patterns are, however, quite different from the powder diagram calculated from the single-crystal X-ray data for $[(\mathrm{Me_3Sn})_2\mathrm{MoO_4}]$. This indicates that the size of the R group exerts a notable structure-directing influence, as observed previously for coordination polymers of the type $[(R_3\mathrm{Sn})_3\mathrm{Rh(SCN)_6}]$ ($R = \mathrm{Me}, \mathrm{Et}, n\mathrm{Pr}$, or $n\mathrm{Bu}$) (26).

Spectroscopic data for compounds **1** and **2** are given in Table 1. In the case of $M = \mathrm{Mo}$, the ν and δ (Mo–O) vibrational frequencies are very close to those exhibited by the trimethyltin derivative $[(\mathrm{Me_3Sn})_2\mathrm{MoO_4}]$ (12). These frequencies and also those of the tungsten(VI) analogue are weakly shifted in comparison to those of the "free" $[M\mathrm{O_4}]^{2-}$ ions, and hence the spectra follow the selection rules for T_d symmetry. Both **1** and **2** give rise to one ν(SnC) vibration at 513 $\mathrm{cm^{-1}}$ in the IR and Raman spectra. The ^{119}Sn MAS NMR spectra of **1** and **2** each show two very close singlets, in the range −20 to 20 ppm, suggesting the presence of two slightly nonequivalent sites in the asymmetric units. By contrast, the single-crystal X-ray structure of $[(\mathrm{Me_3Sn})_2\mathrm{MoO_4}]$ revealed only one tin site in the asymmetric unit. The ^{119}Sn chemical shifts are comparable with that measured in solution for the compound $(\mathrm{Me_3Sn})_4(\mathrm{Cp^*\,W(O)})_4(\mu\mathrm{O})_8$ (δ, −7.3), which has a tetrameric structure in which each tin atom has trigonal bipyramidal coordination geometry (16). The materials **1** and **2** give rise to identical yet somewhat complicated ^{13}C CP MAS NMR spectra at room temperature. Four main signals are observed at $\delta = 14.5$ (C_δ), 20.8 (C_α), 26.9 (C_γ), and 28.2 (C_β). Each of these resonances has associated with it some weaker side peaks that may be due to the presence of nonequivalent butyl groups. For comparison, the $\mathrm{Me_3Sn}$ analogue $[(\mathrm{Me_3Sn})_2\mathrm{MoO_4}]$ contains two nonequivalent methyl C atoms in the asymmetric unit. However, only one symmetric signal is observed in the ^{13}C CP MAS NMR spectrum, attributed to the fact that the $\mathrm{Me_3Sn}$ groups rotate freely about the Sn–O–Sn axes on the NMR time scale (12). In the cases of **1** and **2**, the presence of nonequivalent butyl groups is not surprising considering the ^{119}Sn NMR results. It may also be the case that rotation of bulky R_3Sn groups is restricted on steric grounds.

The material $[(n\mathrm{Bu_3Sn})_2\mathrm{MoO_4}]$ (**1**) was further characterized in the solid state by measuring Mo K-edge and Sn K-edge X-ray absorption spectra at room temperature.

TABLE 1

^{119}Sn CP MAS NMR, Infrared, and Raman Data of $[(n\mathrm{Bu_3Sn})_2M\mathrm{O_4}]$ and $\mathrm{Na_2MO_4 \cdot 2H_2O}$

Compound	^{119}Sn (ppm)	$\mathrm{MO_4}$ unit[a] ($\mathrm{cm^{-1}}$)		ν(SnC) ($\mathrm{cm^{-1}}$)	
		IR	Raman	IR	Raman
$[(n\mathrm{Bu_3Sn})_2\mathrm{MoO_4}]$ (**1**)	20.3, 17.9	850	308, 860, 924	513	513
$\mathrm{Na_2MoO_4 \cdot 2H_2O}$	—	822, 869, 901	327, 838, 896	—	—
$[(n\mathrm{Bu_3Sn})_2\mathrm{WO_4}]$ (**2**)	−13.0, −17.2	850	315, 865, 965	513	513
$\mathrm{Na_2WO_4 \cdot 2H_2O}$	—	825, 858, 931	335, 839, 931	—	—

[a] $[(\mathrm{Me_3Sn})_2\mathrm{MoO_4}]$: IR 860; Raman 310, 867, 918 (12).

TABLE 2

Mo *K*-Edge and Sn *K*-Edge EXAFS-Derived Structural Parameters for $[(n\mathrm{Bu_3Sn})_2\mathrm{MoO_4}]$ (1)[a]

Edge	Fit	Atom	*CN*[b]	*r* (Å)	$2\sigma^{2}$[c] (Å^2)	E_f[d] (eV)	*R*[e] (%)
Mo K	A	O	4.0(1)	1.765(2)	0.0023(2)	0.2(5)	25.9
Mo K	B	O	4.0(1)	1.766(2)	0.0023(2)	−0.1(5)	25.5
		Sn	2.0(10)	3.774(19)	0.0189(36)		
Mo K	C	O	4.0(1)	1.765(2)	0.0023(2)	0.2(5)	25.4
		Sn	2.0(10)	4.075(15)	0.0153(27)		
Sn K	D	C	3.5(5)	2.144(4)	0.0073(7)	−9.2(6)	33.7
		O	2.0(6)	2.256(16)	0.0298(65)		
Sn K	E	C	3.5(4)	2.144(4)	0.0071(6)	−9.5(5)	29.6
		O	2.0(6)	2.261(13)	0.0282(52)		
		Mo	1.0(5)	3.759(9)	0.0137(16)		
Sn K	F	C	3.5(4)	2.143(4)	0.0075(7)	−9.1(5)	30.7
		O	2.0(6)	2.253(14)	0.0308(62)		
		Mo	1.0(6)	4.069(10)	0.0130(19)		

[a] Calculated coordination shells and mean interatomic distances for $[(Me_3Sn)_2MoO_4]$ (central atom in italics, coordination number in parentheses): Mo...O = 1.77 Å (4), Mo...Sn = 3.84 Å (4), Mo...C = 3.86 Å (4), Sn...C = 2.10 Å (2), Sn...C = 2.15 Å (1), Sn...O = 2.27 Å (2), Sn...Mo = 3.84 Å (2), Sn...O = 4.48 Å (4). Calculations were performed using the program SEXIE (27) with X-ray single-crystal data taken from Ref. 12. The maximum deviation for considering atoms to be in a common shell, 0.01 Å.

[b] *CN* = Coordination number. Values in parentheses are statistical errors generated in EXCURVE. The true errors in coordination numbers are likely to be on the order of 20%; those for the interatomic distances ca. 1.5% (28).

[c] Debye–Waller factor; σ = root-mean-square internuclear separation.

[d] E_f = Edge position (Fermi energy), relative to calculated vacuum zero.

[e] $R = (\int[\sum^{\mathrm{theory}} - \sum^{\mathrm{exptl}}]k^3\mathrm{d}k/[\sum^{\mathrm{exptl}}]k^3\mathrm{d}k) \times 100\%$.

The Mo *K*-edge extended X-ray absorption fine structure (EXAFS) of **1** was initially fitted by a model comprising four oxygen atoms at 1.77 Å (Table 2, fit A). The refined coordination number (*CN*) and distance match very well with the values determined for $[(Me_3Sn)_2MoO_4]$ by single-crystal X-ray diffraction (see footnote to Table 2). There is only one type of molybdenum atom in the asymmetric unit for the trimethyltin analogue. The second coordination shell for this atom consists of four tin atoms at a mean distance of 3.84 Å. The Fourier transform (FT) of the Mo *K*-edge EXAFS of **1** does indicate the presence of shells around 4 Å (Fig. 2). A second shell for tin was added to the model (*CN* = 2) and a contour plot calculated to show the variation of the fit index with the two interatomic distances Mo...O (1.755–1.775 Å) and Mo...Sn (3.6–4.2 Å). This map clearly indicated the existence of two minima in the fit index corresponding to two different Mo...Sn distances. Least-squares refinement yielded values of 3.77 and 4.08 Å (fits B and C, respectively, Table 2). Figure 2 shows the results obtained with fit B. The existence of these shells would obviously suggest the presence of short and long Mo...Sn interactions, in contrast to the structure of $[(Me_3Sn)_2MoO_4]$ in which four tin atoms are located at 3.84 ± 0.01 Å. However, considerable caution must be attached to the accuracy of these results, as the addition of either of these second shells produces only a relatively small decrease in the goodness-of-fit *R* factor (Table 2). The statistical errors for the refined parameters are also large (50% in coordination number and 19% in Debye–Waller factor).

The Sn *K*-edge EXAFS of **1** was initially fitted by a two-shell model comprising 3.5 carbon atoms at 2.14 Å and 2.0 oxygen atoms at 2.26 Å (Table 2, fit D). This correlates well with the structure of $[(Me_3Sn)_2MoO_4]$ (Table 2) and is consistent with the presence of *trans*-R_3SnO_2 units with trigonal bipyramidal geometry. The Debye–Waller factor for the Sn...O shell is quite large, indicating considerable static or thermal disorder in the Sn–O bond. In the case of the trimethyltin analogue, two carbon atoms bonded to tin are found at 2.095 Å while the third is found at 2.147 Å. Analysis of the EXAFS data for **1** reveals only one uniform Sn...C interaction, at 2.14 Å ($2\sigma^2 = 0.007$ Å^2). This distance is typical of Sn^{IV} coordination polymers containing *trans*-$(n\mathrm{Bu})_3SnO_2$ units, for example tri-*n*-butyltin carboxylates (29). As found for the Mo *K*-edge data, the FT of the Sn *K*-edge EXAFS of **1** indicates the presence of shells around 4 Å (Fig. 2). Considering again the structure of the trimethyltin analogue, there is only one type of tin atom in the asymmetric unit and each of these is surrounded by two molybdenum atoms at a mean distance of 3.84 Å.

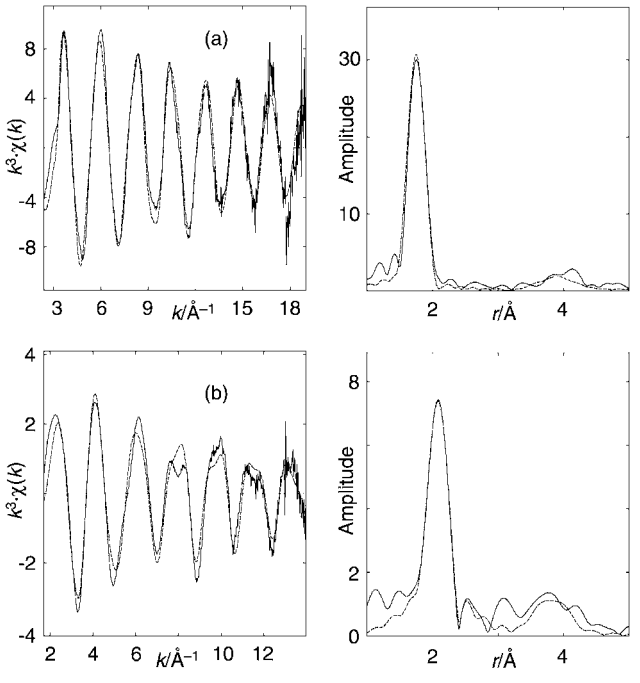

FIG. 2. Mo *K*-Edge (a) and Sn *K*-Edge (b) EXAFS and Fourier transforms of $[(n\mathrm{Bu_3Sn})_2\mathrm{MoO_4}]$ (**1**). The solid lines represent the experimental data and the dashed lines show fits using parameters given in Table 2 (fit B for Mo *K*-edge data and fit E for Sn *K*-edge data).

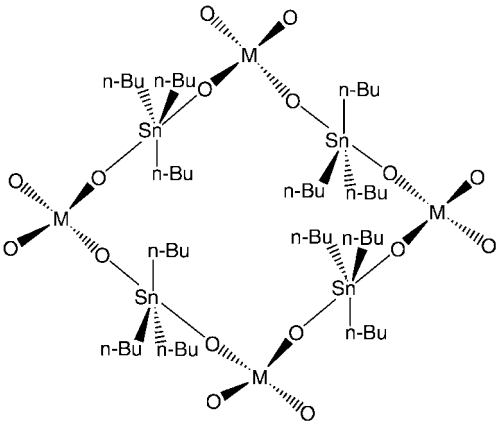

FIG. 3. Representation of proposed structure of one layer in $[(n\mathrm{Bu_3Sn})_2\mathrm{MoO_4}]$ (**1**).

A third shell for molybdenum ($CN = 1$) was added to the fit to the Sn *K*-edge EXAFS of **1** and a contour plot calculated to show the variation of the fit index with the two interatomic distances Sn...C (2.12–2.17 Å) and Sn...Mo (3.6–4.2 Å). As found for the Mo *K*-edge EXAFS data, there were two minima in the fit index corresponding to two different Sn...Mo distances. Full analysis showed in fact that these two distances correlate remarkably well with the values obtained from the Mo *K*-edge EXAFS data (fits E and F, Table 2). Figure 2 shows the results obtained with fit E. Addition of either shell produces a significant improvement in the fit. This seems to be quite a strong confirmation for the presence of short (3.76 Å) and long (4.07 Å) Mo...Sn interactions in **1**. In conclusion, the EXAFS-derived local coordination environment of compound **1** points toward a polymeric layered structure with a framework connectivity analogous to that in $[(\mathrm{Me_3Sn})_2\mathrm{MoO_4}]$ (Fig. 3). There are, however, some subtle differences within the layers, caused by the presence of the *n*-butyl groups. Powder X-ray diffraction also indicates that increase in the size of the *R* groups induces a considerable lattice expansion, presumably in a direction perpendicular to the layers.

Oxidation Catalysis

Molybdenum(VI) compounds are of great importance in catalytic reactions involving oxidation processes (30). The most significant reaction in industry is the epoxidation of propylene to propylene oxide by alkylhydroperoxides, catalyzed with high activity and selectivity by soluble $\mathrm{Mo^{VI}}$ compounds (31). The coordination polymer $[(n\mathrm{Bu_3Sn})_2\mathrm{MoO_4}]$ (**1**) was initially tested as a catalyst or catalyst precursor for the epoxidation of cyclooctene at 55°C, using *tert*-butyl hydroperoxide (TBHP, 70% in decane) as oxidant without additional solvent. A control experiment confirmed that no reaction takes place in the absence of **1**. In the presence of **1**, cyclooctene oxide was formed as the only detectable product with an initial activity of 21 mol $\mathrm{mol^{-1}}$ Mo $\mathrm{h^{-1}}$. The epoxide yield after 24 h was 88%. This activity is comparable with that obtained for *cis*-dioxomolybdenum(VI) complexes of the type $\mathrm{MoO_2}X_m(L)_n$ ($X = \mathrm{Cl, Br, Me}$) under similar reaction conditions (32–35). The important feature of **1** is that it is insoluble under these conditions and therefore the catalysis is, in principle, heterogeneous. Indeed, the coordination polymer was easily separated from the reaction mixture by centrifuging. After thoroughly washing with dichloromethane it was used in a second reaction cycle. The oxidation rate remained roughly the same: initial activity varied from 21 to 27 mol $\mathrm{mol^{-1}}$ Mo $\mathrm{h^{-1}}$ and cyclooctene conversion from 67 to 78% after 24 h (Table 3). This suggests that the organotin–oxomolybdate is not significantly degraded during the oxidative process. These promising results prompted us to examine further the catalytic performance of **1** and also its tungsten analogue **2**. As will be shown, the oxidation results depend on the type of oxidant, the reaction temperature, the solvent, and the nature of the substrate.

Changing the type of oxidant from TBHP to aqueous $\mathrm{H_2O_2}$ does not have a detrimental effect on product selectivity; i.e., cyclooctene oxide is still the only product observed (at 35, 55, or 75°C, Table 3). In sharp contrast to what is usually observed with *cis*-dioxomolybdenum(VI) complexes, use of aqueous $\mathrm{H_2O_2}$ actually improves the catalytic activity of $[(n\mathrm{Bu_3Sn})_2\mathrm{MoO_4}]$ (**1**) under equivalent reaction conditions (from 7 to 179 mol $\mathrm{mol^{-1}}$ Mo $\mathrm{h^{-1}}$ at 55°C, Table 3). The yield is quantitative after 6 h, even when the reaction is carried out at the lower temperature of 35°C. Increasing the reaction temperature from 35 to 75°C increased the initial activity of **1** from 116 to 297 mol $\mathrm{mol^{-1}}$ Mo $\mathrm{h^{-1}}$. The apparent activation energy was estimated from the slope of the Arrhenius plot to be 5 kcal $\mathrm{mol^{-1}}$, which is quite low, suggesting the existence of some mass transfer limitation. Rao *et al.* reported a value of 25.8 kcal $\mathrm{mol^{-1}}$ for the air epoxidation of cyclooctene using

TABLE 3

Influence of the Oxidant on Cyclooctene Epoxidation in the Presence of $[(n\mathrm{Bu_3Sn})_2\mathrm{MoO_4}]$ (1)

Oxidant	Temp. (°C)	Conv. (%)[a]	Initial activity (mol $\mathrm{mol^{-1}}$ Mo $\mathrm{h^{-1}}$)
TBHP (70%, *n*-decane) (1st run)[b]	55	67	21
TBHP (70%, *n*-decane) (2nd run)[b,c]	55	78	26
TBHP (70% aqueous)[d]	55	27	7
$\mathrm{H_2O_2}$ (30% aqueous)[d]	35	100	116
$\mathrm{H_2O_2}$ (30% aqueous)[d]	55	100	179
$\mathrm{H_2O_2}$ (30% aqueous)[d]	75	100	297

[a] After 7 h.
[b] No additional solvent.
[c] After centrifugation, washing, and drying.
[d] 1,2-Dichloroethane as additional solvent.

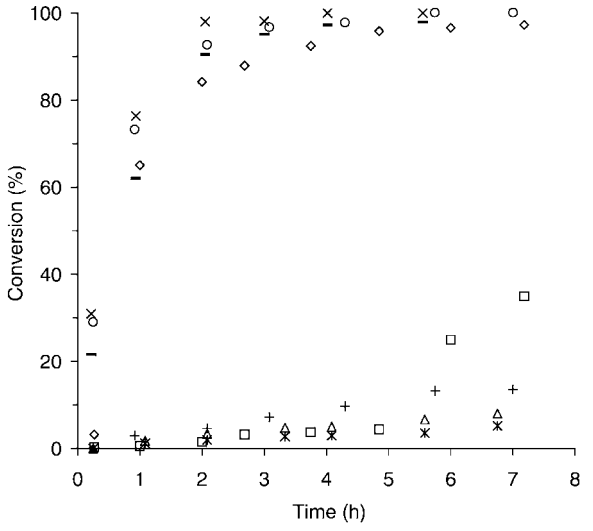

FIG. 4. Influence of the type of solvent on cyclooctene conversion, using H_2O_2 in the presence of $[(n\mathrm{Bu_3Sn})_2\mathrm{MoO_4}]$ (**1**), at 35°C: ◇, no additional solvent; ○, 1,2-dichloroethane; ×, dichloromethane; □, water; +, acetonitrile; △, ethanol; ∗, methanol; −, dichloromethane plus radical scavenger.

cis-[MoO_2(salicylidene salicyloyl hydrazinato-)(solv)] in the same temperature range (36). Previous kinetic and spectroscopic studies have shown that the mechanism of olefin epoxidation in the case of $MoO_2X_m(L)_n$ complexes using TBHP involves *in situ* formation of an oxidizing agent by coordination of TBHP to the Mo center, generating an OO*R* group as a seventh ligand (37). The addition of a radical scavenger at the beginning of the reaction with **1** and H_2O_2 (equimolar amounts of cyclooctene and 2,6-di-*tert*-butyl-4-methyl-phenol) does not affect significantly the catalytic activity, suggesting that a nonradical reaction mechanism is involved (Fig. 4). These results suggest that H_2O_2 reacts with the polymer to give an oxidizing species that is more reactive for cyclooctene epoxidation than those formed from TBHP.

At 35°C and using aqueous H_2O_2 as oxidant, changing the type of additional solvent does not result in products other than cyclooctene oxide (Fig. 4). On the other hand, the initial activity of $[(n\mathrm{Bu_3Sn})_2\mathrm{MoO_4}]$ (**1**) does depend on the solvent and increases in the following order: methanol < water < ethanol < acetonitrile < no additional solvent < 1,2-dichloroethane < dichloromethane (Table 4). The system is homogeneous in the case of ethanol, methanol, and acetonitrile and triphasic [aqueous (H_2O_2/H_2O) + organic (cyclooctene) + solid (**1**)] with the chloride solvents, with water, or without additional solvent. The best results are obtained with chloride solvents, which are noncoordinating (heterogeneous system): the epoxide is obtained in quantitative yields after 6 h (Table 4). When coordinating solvents are used, conversion is less than 14% at this stage of the reaction. Without additional solvent cyclooctene conversion is >96%. In the case of water, an induction period of approximately 5 h is observed, after which conversion increases rapidly up to 96% after 24 h. It is possible that the coordinating solvent molecules compete with peroxide for coordination to the molybdenum center, thus decreasing cyclooctene conversion.

An attempt to verify if any dissolved catalyst in 1,2-dichloroethane contributes to the observed activity was made by carrying out an experiment in which, first of all, compound **1**, solvent, and oxidant were mixed at 35°C. After 15 min the solid material was separated by centrifugation, and cyclooctene was added to the supernatant solution and allowed to react under standard conditions. Cyclooctene epoxidation takes place, but the initial reaction rate (ca. 5 mol mol^{-1} Mo h^{-1}) is much lower than that observed in the normal catalytic system with **1** (116 mol mol^{-1} Mo h^{-1}). This residual activity may be due to a small amount of dissolved catalyst species, or alternatively to colloidal particles in solution that were not fully removed by the separation process.

The catalytic performance of $[(n\mathrm{Bu_3Sn})_2\mathrm{MoO_4}]$ (**1**) for cyclooctene epoxidation was compared with that for other substrates, namely bulky cyclic (cyclododecene) and linear (1-octene, 2-octene) olefins. In order to exclude solvent effects on the reaction no additional solvent was used. After a 6-h reaction, no 1-octene conversion was observed, whereas in the case of 2-octene 52% conversion was attained (100% selectivity toward the epoxide). The apparent higher reactivity toward internal C=C double bonds in comparison to the terminal ones may be due to the higher electron density of the former. It is possible that relative reactivities depend mainly on the nucleophilicity of the double bond (38). The initial activity for the epoxidation of cyclododecene (6 mol mol^{-1} Mo h^{-1}) was less than a third of that observed for cyclooctene (21 mol mol^{-1} Mo h^{-1}). This may be due to steric hindrance, which occurs to a greater extent in the case of the bulkier olefin.

The tungsten(VI) analogue $[(n\mathrm{Bu_3Sn})_2\mathrm{WO_4}]$ (**2**) is considerably less active than $[(n\mathrm{Bu_3Sn})_2\mathrm{MoO_4}]$ (**1**) for the

TABLE 4

Influence of the Solvent on Cyclooctene Epoxidation with 30% Aqueous H_2O_2 in the Presence of $[(n\mathrm{Bu_3Sn})_2\mathrm{MoO_4}]$ (1) at 35°C

Solvent	Conv.[a] (%)	Initial activity (mol mol^{-1} Mo h^{-1})	Phase system[b]
Water	25	1.3	L–L–S
Methanol	≤6	1.1	L
Ethanol	≤8	1.6	L
Acetonitrile	≤14	3.3	L
1,2-Dichloroethane	100	116	L–L–S
Dichloromethane	100	179	L–L–S
No solvent	97	11.9	L–L–S

[a] After 6 h.

[b] L = Organic or aqueous phase, S = solid phase (catalyst).

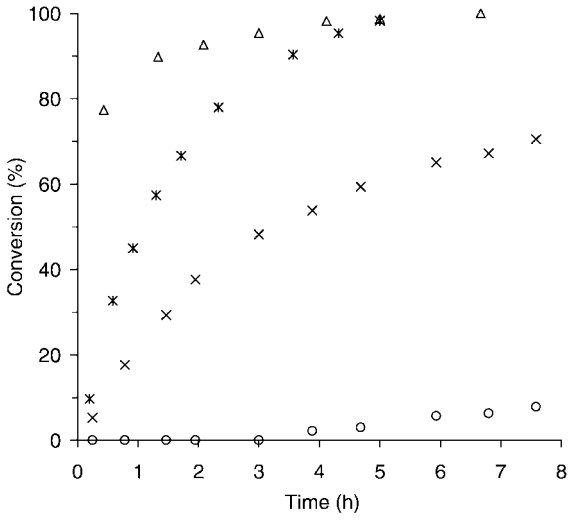

FIG. 5. Cyclooctene conversion using TBHP (70% in *n*-decane) or aqueous H_2O_2 (30%) at 55°C in the presence of $[(n\mathrm{Bu_3Sn})_2\mathrm{MoO_4}]$ (**1**) (×, TBHP; △, H_2O_2) or $[(n\mathrm{Bu_3Sn})_2\mathrm{WO_4}]$ (**2**) (○, TBHP; ⁎, H_2O_2).

catalytic epoxidation of cyclooctene by TBHP (70%, *n*-decane) at 55°C (no additional solvent). Thus, in the presence of **2**, an induction period of 3 h is observed and after 24-h conversion reaches only 30% (Fig. 5). This difference in activity is not surprising when one considers previous work that compares the activities of oxotungsten(VI) and oxomolybdenum(VI) complexes. For example, in a recent study of chiral 2′-pyridinyl alcoholate complexes of the type MO_2L_2, the tungsten(VI) complexes were found to have markedly lower activities than the molybdenum(VI) complexes for the enantioselective epoxidation of *trans*-methylstyrene by TBHP (39). It is interesting that for compound **2**, when aqueous H_2O_2 (30%) is used as oxidant at 55°C with 1,2-dichloroethane as additional solvent, catalytic activity increases remarkably (Fig. 5). Initial activity continues nevertheless to be lower than that of the molybdenum analogue. However, for both compounds, cyclooctene epoxide is obtained in quantitative yield after 5 h. The WO_3 metal oxides are known to catalyze reactions of hydrogen peroxide through the formation of peracids, which can interact with alkenes, yielding the corresponding epoxide (40).

CONCLUSIONS

Materials with the general formula $[(R_3\mathrm{Sn})_2MO_4]$ (M = Mo, W) possess a polymeric layered structure where small variations can be introduced by changing the nature and bulk of the R substituent. In this work we have shown that the compounds with $R = n\mathrm{Bu}$ are active catalysts/catalyst precursors for the epoxidation of olefins with either TBHP/decane or aqueous 30% H_2O_2 as oxidant. The latter system is significantly more active and both are very selective in the formation of the epoxide. The higher activities were found for triphasic systems (aqueous H_2O_2/organic chlorinated solvent/solid catalyst). The molybdenum catalysts are clearly superior to the tungsten ones. Following these observations, further studies are aimed at understanding what effect changing the nature and size of R groups has on the catalytic activity/selectivity.

ACKNOWLEDGMENTS

This work was mainly funded by FCT, POCTI, and PRAXIS XXI (including a Ph.D. grant to M.A. and postdoctoral grants to A.A.V. and M.P.). We acknowledge the European Synchrotron Radiation Facility for provision of synchrotron radiation facilities and we thank Stuart Ansell for assistance in using the beamline BM29.

REFERENCES

1. Janiak, C., *Angew. Chem. Int. Ed. Engl.* **36**, 1431 (1997).
2. Yaghi, O. M., Li, H. L., Davis, C., Richardson, D., and Groy, T. L., *Acc. Chem. Res.* **31**, 474 (1998).
3. Blake, A. J., Champness, N. R., Hubberstey, P., Li, W. S., Withersby, M. A., and Schroder, M., *Coord. Chem. Rev.* **183**, 117 (1999).
4. Eddaoudi, M., Moler, D. B., Li, H. L., Chen, B. L., Reineke, T. M., O'Keeffe, M., and Yaghi, O. M., *Acc. Chem. Res.* **34**, 319 (2001).
5. Niu, T., and Jacobson, A. J., *Inorg. Chem.* **38**, 5346 (1999).
6. Niu, T., Lu, J., Wang, X., Korp, J. D., and Jacobson, A. J., *Inorg. Chem.* **37**, 5324 (1998).
7. Lu, J., Harrison, W. T. A., and Jacobson, A. J., *Angew. Chem. Int. Ed. Engl.* **34**, 2557 (1995).
8. Behrens, U., Brimah, A. K., and Fischer, R. D., *J. Organomet. Chem.* **411**, 325 (1991).
9. Behrens, U., Brimah, A. K., Soliman, T. M., Fischer, R. D., Apperley, D. C., Davies, N. A., and Harris, R. K., *Organometallics* **11**, 1718 (1992).
10. Brandt, P., Brimah, A. K., and Fischer, R. D., *Angew. Chem. Int. Ed. Engl.* **27**, 1521 (1988).
11. Schwarz, P., Eller, S., Siebel, E., Soliman, T. M., Fischer, R. D., Apperley, D. C., Davies, N. A., and Harris, R. K., *Angew. Chem. Int. Ed. Engl.* **35**, 1525 (1996).
12. Behrens, U., Brimah, A. K., Yünlü, K., and Fischer, R. D., *Angew. Chem. Int. Ed. Engl.* **32**, 82 (1993).
13. Herdtweck, E., Kiprof, P., Herrmann, W. A., Kuchler, J. G., and Degnan, I., *Z. Naturforsch. B Chem. Sci.* **45**, 937 (1990).
14. Kanellakopulos, B., Raptis, K., Nuber, B., and Ziegler, M. L., *Z. Naturforsch. B Chem. Sci.* **46**, 15 (1991).
15. Rosenland, F., and Merzweiler, K., *Z. Anorg. Allg. Chem.* **627**, 2403 (2001).
16. Rau, M. S., Kretz, C. M., Geoffroy, G. L., Rheingold, A. L., and Haggerty, B. S., *Organometallics* **13**, 1624 (1994).
17. Niwa, M., Yamada, H., and Murakami, Y., *J. Catal.* **134**, 331 (1992).
18. Niwa, M., Sano, M., Yamada, H., and Murakami, Y., *J. Catal.* **151**, 285 (1995).
19. Valente, N. G., Cadús, L. E., Gorriz, O. F., Arrúa, L. A., and Rivarola, J. B., *Appl. Catal. A* **153**, 119 (1999).
20. Lakshmi, L. J., and Alyea, E. C., *Catal. Lett.* **59**, 73 (1999).
21. Ono, T., Kamisuki, H., Hisashi, H., and Miyata, H., *J. Catal.* **116**, 303 (1989).
22. Allakhverdova, N. Kh., Adzhamov, K. Yu., and Alkhazov, T. G., *Kinet. Katal.* **33**, 327 (1992).
23. Medeiros, P. R. S., Eon, J. G., and Appel, L. G., *Catal. Lett.* **69**, 79 (2000).
24. Binsted, N., EXCURV98, CCLRC Daresbury Laboratory computer programme, 1998.

25. Gurman, S. J., Binsted, N., and Ross, I., *J. Phys. C* **17**, 143 (1984); **19**, 1845 (1986).
26. Siebel, E., and Fischer, R. D., *Chem. Eur. J.* **3**, 1987 (1997).
27. Rupp, B., Smith, B., and Wong, J., *Comp. Phys. Commun.* **67**, 543 (1992).
28. Evans, J., Gauntlett, J. T., and Mosselmans, J. F. W., *Faraday Discuss. Chem. Soc.* **89**, 107 (1990).
29. Ng, S. W., Kumar Das, V. G., and Tiekink, R. T., *J. Organomet. Chem.* **411**, 121 (1991).
30. Jorgensen, K. A., *Chem. Rev.* **89**, 431 (1989).
31. Sheldon, R. A., Wallau, M., Arends, I. W. C. E., and Schuchardt, U., *Acc. Chem. Res.* **31**, 485 (1998).
32. Kühn, F. E., Herdtweck, E., Haider, J. J., Herrmann, W. A., Gonçalves, I. S., Lopes, A. D., and Romão, C. C., *J. Organomet. Chem.* **583**, 3 (1999).
33. Kühn, F. E., Lopes, A. D., Santos, A. M., Herdtweck, E., Haider, J. J., Romão, C. C., and Santos, A. G., *J. Mol. Catal. A.* **151**, 147 (2000).
34. Kühn, F. E., Santos, A. M., Lopes, A. D., Gonçalves, I. S., Herdtweck, E., and Romão, C. C., *J. Mol. Catal. A* **164**, 25 (2000).
35. Ferreira, P., Gonçalves, I. S., Kühn, F. E., Lopes, A. D., Martins, M. A., Pillinger, M., Pina, A., Rocha, J., Romão, C. C., Santos, A. M., Santos, T. M., and Valente, A. A., *Eur. J. Inorg. Chem.* 2263 (2000).
36. Rao, S. N., Munshi, K. N., and Rao, N. N., *J. Mol. Catal. A* **145**, 203 (1999).
37. Thiel, W. R., and Eppinger, J., *Chem. Eur. J.* **3**, 696 (1997).
38. Deng, Y., and Maier, W. F., *J. Catal.* **199**, 115 (2001).
39. Herrmann, W. A., Haider, J. J., Fridgen, J., Lobmaier, G. M., and Spiegler, M., *J. Organomet. Chem.* **603**, 69 (2000).
40. Mudgan, M., and Young, D. P., *J. Chem. Soc.* 2988 (1949).